Original Article

Split-filter dual-energy CT pulmonary angiography for the diagnosis of acute pulmonary embolism: a study on image quality and radiation dose

Bernhard Petritsch^, Pauline Pannenbecker^, Andreas M. Weng^, Jan-Peter Grunz^, Simon Veldhoen^, Thorsten A. Bley^, Aleksander Kosmala^

Department of Diagnostic and Interventional Radiology, University Hospital Würzburg, Würzburg, Germany

Correspondence to: Dr. Bernhard Petritsch, MD. Department of Diagnostic and Interventional Radiology, University Hospital Würzburg, Oberdürrbacherstr. 6, D-97080 Würzburg, Germany. Email: petritsch_b@ukw.de.

Background: Computed tomography (CT) pulmonary angiography is the diagnostic reference standard in suspected pulmonary embolism (PE). Favorable results for dual-energy CT (DECT) images have been reported for this condition. Nowadays, dual-energy data acquisition is feasible with different technical options, including a single-source split-filter approach. Therefore, the aim of this retrospective study was to investigate image quality and radiation dose of thoracic split-filter DECT in comparison to conventional single-energy CT in patients with suspected PE.

Methods: A total of 110 CT pulmonary angiographies were accomplished either as standard single-energy CT with automatic tube voltage selection (ATVS) (n=58), or as split-filter DECT (n=52). Objective [pulmonary artery CT attenuation, signal-to-noise ratio (SNR), contrast-to-noise ratio (CNR)] and subjective image quality [four-point Likert scale; three readers (R)] were compared among the two study groups. Size-specific dose estimates (SSDE), dose-length-product (DLP) and volume CT dose index (CTDIvol) were assessed for radiation dose analysis.

Results: Split-filter DECT images yielded 67.7% higher SNR (27.0 *vs.* 16.1; P<0.001) and 61.9% higher CNR (22.5 *vs.* 13.9; P<0.001) over conventional single-energy images, whereas CT attenuation was significantly lower (344.5 *vs.* 428.2 HU; P=0.013). Subjective image quality was rated good or excellent in 93.0%/98.3%/77.6% (R1/R2/R3) of the single-energy CT scans, and 84.6%/82.7%/80.8% (R1/R2/R3) of the split-filter DECT scans. SSDE, DLP and CTDIvol were significantly lower for conventional single-energy CT compared to split-filter DECT (all P<0.05), which was associated with 26.7% higher SSDE.

Conclusions: In the diagnostic workup of acute PE, the split-filter allows for dual-energy data acquisition from single-source single-layer CT scanners. The existing opportunity to assess pulmonary "perfusion" based on analysis of iodine distribution maps is associated with higher radiation dose in terms of increased SSDE than conventional single-energy CT with ATVS. Moreover, a proportion of up to 3.8% non-diagnostic examinations in the current reference standard test for PE is not negligible.

Keywords: Dual-energy; CT-angiography; vascular; pulmonary arteries; embolism/thrombosis

Submitted Jun 08, 2020. Accepted for publication Nov 26, 2020.
doi: 10.21037/qims-20-740
View this article at: http://dx.doi.org/10.21037/qims-20-740

^ ORCID: Bernhard Petritsch, 0000-0002-9909-1592; Paulina Pannenbecker, 0000-0002-2811-9316; Andreas M. Weng, 0000-0001-8943-3539; Jan-Peter Grunz, 0000-0002-4524-1620; Simon Veldhoen, 0000-0002-3585-5442; Thorsten A. Bley, 0000-0001-9311-7985; Aleksander Kosmala, 0000-0002-9313-9356.

Introduction

Pulmonary embolism (PE) represents a serious and frequent cardiovascular disease, potentially leading to acute or chronic life-threatening complications (1). Mortality and morbidity are significantly reduced when therapy is initiated promptly. Therefore a timely and clear diagnosis is crucial (2,3). Computed tomography pulmonary angiography (CTPA) is regarded as reference standard for diagnostic imaging in patients with suspected PE, offering short examination times, high sensitivity, and high specificity (4-7).

The roll out of dual-source CT (DSCT) scanners led to a revival of dual-energy CT (DECT), adding functional imaging information (8,9) by illustration of pulmonary perfusion defects with a good agreement compared to V/Q scans (10). Thereby absorption characteristics of materials with comparatively high atomic numbers, for example iodine ($_{53}$I), can be depicted by simultaneously using a low and a high tube energy (kV) (11). Although the greatest number of dual-energy CTPA studies has been performed on DSCT scanners, all major CT vendors offer dual-energy opportunities on their high-end scanners, based on different technical approaches (e.g., dual-layer, Philips Healthcare; rapid kVp switching, GE Healthcare; sequential DECT, Canon Medical Systems Corporation) (12,13). The various advantages, possibilities, but also limitations of dual-energy imaging in the context of suspected PE have been discussed and published before (14-17). Studies regarding image quality and radiation dose of CTPA scans performed on various generations of dual-source scanners report promising results: DECT is proven to carry a similar or even lower radiation dose compared to conventional single-source CT, while providing at least comparable image quality and potential complimentary information by computation of dual-energy iodine distribution maps (18-20). It has been shown that iodine maps indeed offer incremental benefits for the detection of occlusive peripheral pulmonary emboli (14).

Recently, a new technical approach for acquiring a dual-energy dataset from a single-source scanner by using a split-filter (SF) (TwinBeam Dual-Energy, Siemens Healthineers) has been introduced. Although the principle of the method has already been propagated in 1980, the first clinical scanner became available much later in 2014 (21). The split filter consists of a gold part (Au) and a tin part (Sn) and is positioned next to the X-ray tube to split the X-ray beam (typically 120 kVp) into two different spectra. Thereby the gold-component of the filter produces a comparatively low-energy spectrum of mean 68 keV, whereas the tin-component of the filter achieves a high-energy spectrum output of mean 86 keV (22). To date, data regarding image quality and associated radiation exposure of split-filter protocols are available only for thoracoabdominal CT scans for oncologic staging and head and neck imaging (22-24). However, the use of a split-filter in CTPA should enable optimized noise levels and computation of iodine perfusion maps at a radiation dose similar to standard single-energy CT.

Thus, the purpose of this study was to investigate image quality and radiation dose parameters of split-filter DECT in comparison to standard single-energy CT in patients with suspected PE.

Methods

This Health Insurance Portability and Accountability Act (HIPAA) compliant study was approved by our institutional review board (IRB). Since all CT-scans were clinically indicated the need for individual informed consent was waived by the IRB. We retrospectively evaluated 110 patients who underwent CTPA between for work-up of suspected acute PE before (September 2018 to December 2019) and after (January 2019 to May 2019) induction of the split-filter technique. From the overall 110 patients 58 patients were scanned with standard single-energy CT mode (study group 1) and 52 patients were scanned with dual-energy CT mode by using the split-filter (study group 2). The patient's demographics, including body habitus parameters (lateral, anteroposterior and effective chest diameter) are summarized in *Table 1*.

CT image acquisition

All CT examinations were performed on a clinical 128-row single-source scanner (SOMATOM Definition Edge, Siemens Healthineers) equipped with the before mentioned split-filter and a single-layer detector (Stellar, Siemens Healthineers). CT scans in the standard single-energy CT group were performed with automatic tube voltage selection (ATVS) (CARE kV, Siemens Healthineers) and automatic tube current modulation (CARE Dose 4D, Siemens Healthineers) (*Figure 1A*). The ATVS selected 80 kV in 28 patients, 100 kV in 28 patients, and 120 kV in 2 patients. SF-DECT acquisitions were performed with default settings at a fixed tube voltage of 120 kV. The dual-energy data is acquired by inserting the combined gold (Au; 0.05 mm)-tin (Sn; 0.6 mm) filter with each 50% coverage

Table 1 Patient demographics

Characteristics	Study group 1, standard CT	Study group 2, split-filter DECT	P value
Patients (n)	58	52	–
Male (n)/female (n)	28/30	26/26	–
Age (±SD), years	65.0 (±17.9)	68.2 (±14.1)	0.313
lateral chest diameter (±SD), cm	35.6 (±5.6)	34.5 (±4.7)	0.177
AP chest diameter (±SD), cm	25.9 (±3.4)	25.4 (±3.6)	0.454
effective chest diameter (±SD), cm	30.2 (±3.5)	29.5 (±3.8)	0.295

DECT, dual-energy computed tomography; AP, anteroposterior; SD, standard deviation.

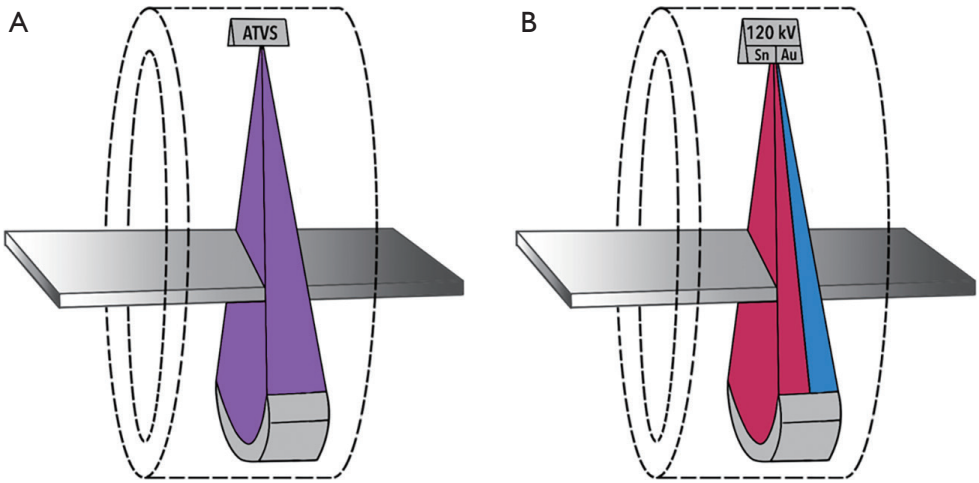

Figure 1 Operation of a single-source CT scanner in standard single-energy mode (A) with automated tube voltage selection (ATVS) and in dual-energy mode (B) using a novel split-filter consisting of a gold (Au) and a tin (Sn) part.

in *z*-axis and full FOV coverage (50 cm) (*Figure 1B*). Due to absorption of low-energy photons by the tin part of the filter, the X-ray spectrum is shifted towards higher energies (*Figure 2*). To enable accurate data acquisition from each voxel at both energy levels, the pitch factor is limited to 0.25 when the split-filter is in use. Detailed scan parameters for both CT protocols are summarized in *Table 2*.

CT scans were performed in caudo-cranial direction between the lung apices and costophrenic recesses in inspiration. The scan length in *z*-axis was recorded. Transverse iterative image reconstructions (ADMIRE, Siemens Healthineers) were performed at 3 mm a slice thickness and use of a medium soft kernel (I40F/Q40F). In study group 2, three image stacks were reconstructed for each patient: one image series for the low (Au) and the high (Sn) energy level each, and one linear blended series in order to resemble an image impression and attenuation characteristics similar to a standard polychromatic 120 kV examination.

An iodinated contrast agent with 350 mg/mL (Imeron® 350, Bracco) was delivered into an antecubital vein by an automated injector (60 mL, 4 mL/s in study group 1; 80 mL, 5 mL/s in study group 2) followed by a 40 mL NaCl chaser bolus. Real-time bolus tracking (CARE Bolus, Siemens Healthineers) was applied with a pulmonary artery trigger attenuation of 120 HU and a delay preceding image acquisition of 5 seconds (study group 1) or 7 seconds (study group 2), respectively.

Objective image quality analysis

CT attenuation in Hounsfield units (HU) and image noise

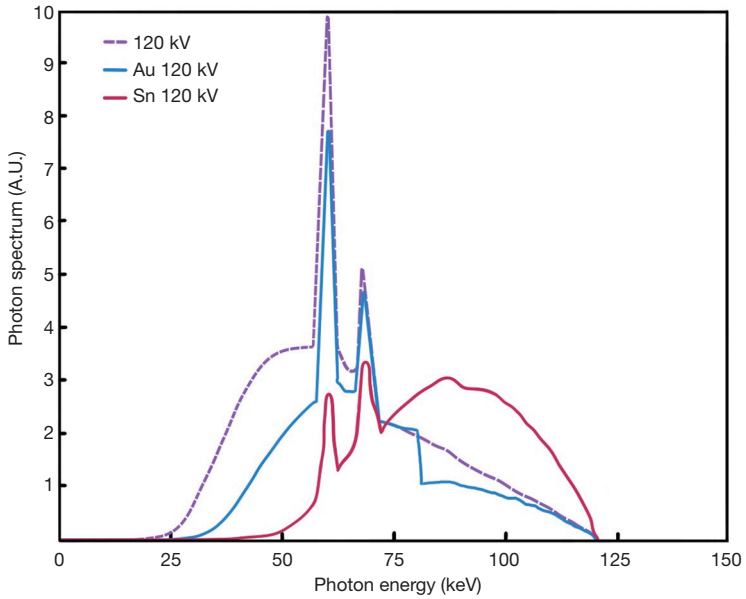

Figure 2 Illustration of three different X-ray spectra at 120 kV: no filtration (dotted purple line); with gold (Au) filtration (blue line representing low-energy spectrum); with tin (Sn) filtration (red line representing high-energy spectrum). The Sn filter shifts the polychromatic X-ray spectrum towards higher photon energies, which is known as spectral shaping [according to Euler *et al.* (23)].

[defined as standard deviation of the CT attenuation of the individual region of interest (ROI)] were obtained by placing circular ROIs at four different intravascular locations (bifurcation of the pulmonary trunk, right lower lobe artery, left upper lobe artery, descending aorta at the level of pulmonary trunk bifurcation) by one reader (radiology internship student, little CT experience). In case of PE of the respecting vessel, HU measurements were derived from the corresponding contralateral vessel. In addition, the muscle density (in HU) was determined from the erector spinae muscles. In study group 2 all measurements and image quality ratings were accomplished in the blended image series. Subsequently, the signal-to-noise ratio (SNR) and the contrast-to-noise ratio (CNR) were calculated using the following equations:

$$SNR = \frac{ROI\left(mean\,HU\right)}{Image\,noise\left(SD\,of\,HU\right)} \quad [1]$$

$$CNR = \frac{ROI\left(mean\,HU\right) - Muscle\left(mean\,HU\right)}{Image\,noise\left(SD\,of\,HU\right)} \quad [2]$$

Subjective image quality analysis

All 110 CTPA scans were evaluated independently based on a four-point Likert scale by three observers with varying levels of expertise (reader 1 and reader 2, with 10 and 6 years of experience in cardiovascular imaging, respectively) and the radiology internship student who also obtained the objective image parameters (reader 3). Readers were blinded to the acquisition protocol. A score of 1 (excellent image quality and excellent diagnostic confidence down to the peripheral branches, no motion artifacts, no relevant subjective image noise) represented the best rating, followed by a score of 2 (good image quality and good diagnostic confidence down to sub-segmental level, minor motion artifacts, little subjective image noise), a score of 3 (moderate to poor image quality with practicable evaluation to at least segmental level, severe motion artifacts, high subjective image noise, still of diagnostic quality), and a score of 4 (non-diagnostic image quality) as the worst rating.

Radiation dose evaluation

The volume CT dose index ($CTDI_{vol}$) and the dose-length-product (DLP) were obtained from the standardized dose report provided by the scanner. Size specific dose estimates (SSDE) were calculated to account for individual patient habitus as described before (25).

Table 2 Technical parameters of applied single- and dual-energy CT protocols

Parameters	Study group 1, standard CT	Study group 2, split-filter DECT
CT mode	Single-source	Single-source
	Single-energy	Dual-energy
Collimation	64×0.6 mm (with z-flying focal spot)	64×0.6 mm
Rotation time, s	0.55 s	0.28 s
Pitch	1.7	0.25
Automatic tube current modulation (CARE Dose 4D, Siemens)	On	On
Automatic tube potential control (CARE kV, Siemens)	On	Off
Tube potential (ref.), kV	80 kV	120 kV with Au/Sn filter
Tube current time product (ref.), mAs	157 mAs	211 mAs

DECT, dual-energy computed tomography; Au, gold; Sn, tin.

Statistical analysis

Statistical analysis was performed using dedicated software (SPSS Statistics for windows, version 25, IBM). Ordinal variables were compared using the Mann-Whitney *U* test for independent samples and are presented as means with corresponding standard deviation. Subjective ratings were compared using parametric testing as proposed by Sullivan *et al*. (26) and are presented as absolute numbers and frequencies. The inter-reader reliability for subjective image quality ratings was calculated with the intraclass correlation coefficient (two-way random effect model testing for consistency) and interpreted according to Koo *et al*. (27). A P value ≤0.05 was considered statistically significant.

Results

The age and body habitus (expressed by three differently defined chest diameters) did not differ between the study groups (age P=0.313; lateral diameter P=0.177; anteroposterior diameter P=0.454; eff. diameter P=0.295) (*Table 1*). The mean age across the whole study population of 110 individuals was 66.5 years (56 females). The mean scan length was similar between both study groups (P=0.440). Based on the radiology report, PE was diagnosed in 19.1% of the patients (study group 1, n=16; study group 2, n=5).

Objective image quality

The pulmonary trunk attenuation was significantly higher in study group 1 (428.2±26.5 HU) compared to study group 2 (344.5±12.9 HU; P<0.05) while the corresponding SNR (16.1±4.6 *vs.* 27.0±8.2; P<0.05) and CNR (13.9±4.6 *vs.* 22.5±8.0; P<0.05) were significantly higher in study group 2. Regarding measurements of the right lower lobe artery and the left upper lobe artery, results were comparable to those in the pulmonary trunk. For the descending aorta, the attenuation (223.9±22.9 *vs.* 273.9±11.5), and the SNR and CNR were significantly higher in study group 2 (all P<0.05). Detailed data is summarized in *Table 3*.

Subjective image quality

Subjective image quality was valuated as good or excellent in 93.0%/98.3%/77.6% (R1/R2/R3) of the standard CT scans, and 84.6%/82.7%/80.8% of the SF-DECT scans (*Figure 3*). In study group 2 there were two non-diagnostic scans (one scan in study group 2 was scored as non-diagnostic (=4) by two readers and another scan was scored as non-diagnostic by one reader). In study group 1 no non-diagnostic scan occurred. Statistical analysis revealed no differences between the two study groups for readers 1 and 3 (P=0.1913 for reader 1; P=0.1255 for reader 3), whereas reader 2 preferred image quality of study group 1 (P=0.0083).

Regarding the overall subjective image quality, a single measure intraclass correlation coefficient of 0.828 (95% CI, 0.661–0.903; P<0.001) reflected good to excellent interobserver reliability. An overview of the scores is presented in *Table 4*.

Radiation dose

The mean $CTDI_{vol}$ and DLP [P<0.001 (CTDI); P=0.005

Table 3 Objective image quality

Variables	Study group 1, standard CT	Study group 2, split-filter DECT	P value
Pulmonary trunk (±SD)			
CT attenuation (HU)	428.2 (±26.5)	344.5 (±12.9)	0.013
SNR	16.1 (±4.6)	27.0 (±8.2)	<0.001
CNR	13.9 (±4.6)	22.5 (±8.0)	<0.001
Right lower lobe (±SD)			
CT attenuation (HU)	366.4 (±29.0)	327.3 (±13.3)	0.216
SNR	14.4 (±6.2)	25.6 (±11.9)	<0.001
CNR	12.2 (±5.9)	21.2 (±11.4)	<0.001
Left upper lobe (±SD)			
CT attenuation (HU)	365.3 (±36.9)	305.1 (±14.5)	0.031
SNR	12.3 (±7.6)	23.7 (±12.9)	<0.001
CNR	10.4 (±7.0)	19.2 (±11.8)	<0.001
Descending aorta (±SD)			
CT attenuation (HU)	223.9 (±22.9)	273.9 (±11.5)	0.001
SNR	9.9 (±4.5)	24.2 (±6.8)	<0.001
CNR	7.4 (±4.4)	19.3 (±6.4)	<0.001

Values provided as averages and standard deviations. DECT, dual-energy computed tomography; SNR, signal-to-noise ratio; CNR, contrast-to-noise ratio; SD, standard deviation.

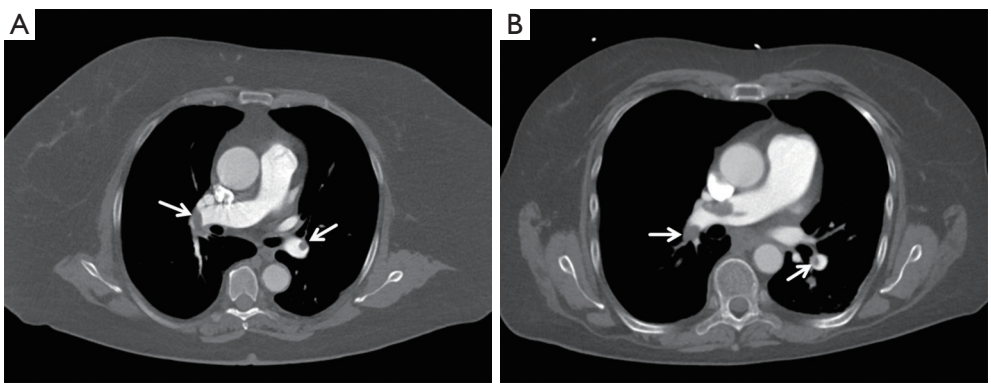

Figure 3 Comparison of axial conventional single-energy image (A) and axial blended split-filter dual-energy image (B) in patients with bilateral pulmonary embolism (arrows). Both scans were rated as excellent (=1) by all three readers.

(DLP)], as well as SSDE (P<0.001) were all significantly lower in the standard CT group compared to the SF-DECT group. In detail, SSDE was 4.53±1.70 mGy (range, 2.32–11.94 mGy) for study group 1 and 5.74±1.06 mGy (range, 3.92–8.28 mGy) for study group 2. All detailed dose index values are given in *Table 5*.

Discussion

In the present study, we for the first time compared "TwinBeam" dual-energy *vs.* standard single-energy image acquisition for CTPA. The achieved subjective diagnostic image quality was rated equal to standard single-energy CT by two of the three readers. However, one reader

Table 4 Subjective image quality

Likert scale	Study group 1, standard CT			Study group 2, split-filter DECT		
	R1	R2	R3	R1	R2	R3
1	40 (68.9%)	49 (84.5%)	15 (25.9%)	32 (61.5%)	36 (69.2%)	23 (44.2%)
2	14 (24.1%)	8 (13.8%)	30 (51.7%)	12 (23.1%)	7 (13.5%)	19 (36.6%)
3	4 (7.0%)	1 (1.7%)	13 (22.4%)	7 (13.5%)	7 (13.5%)	10 (19.2%)
4	–	–	–	1 (1.9%)	2 (3.8%)	–
Median	1	1	2	1	1	2

Values displayed as frequencies and percentage in parenthesis. DECT, dual-energy computed tomography; Likert scale 1, excellent image quality (IQ), 2, good IQ, 3, moderate to poor IQ, 4, non-diagnostic IQ.

Table 5 Radiation dose parameters of CTPA

Parameters	Study group 1, standard CT	Study group 2, split-filter DECT	P value
Scan length (±SD), mm	318 (±34)	310 (±39)	0.440
CTDIvol (±SD), mGy	3.87 (±2.01)	4.72 (±1.50)	<0.001
DLP (±SD), mGy*cm	140.5 (±75.9)	158.9 (±51.4)	0.005
SSDE (±SD), mGy	4.53 (±1.70)	5.74 (±1.06)	<0.001

CTPA, computed tomography pulmonary angiography; DECT, dual-energy computed tomography; CTDIvol, volume computed tomography dose index; DLP, dose-length product; SSDE, size specific dose estimates; SD, standard deviation.

preferred image impression of the standard single-energy CT protocol. Moreover, 2 out of 52 SF-DECT scans (3.8%) were rated as non-diagnostic by at least one reader. This was most likely due to the lower pitch used in the dual-energy study group (0.25 *vs.* 1.7), that leads to a prolonged breath hold time, which can be problematic particularly in elderly and patients with dyspnea. Although the main pulmonary artery enhancement was significantly lower in the dual-energy study group, there was still adequate enhancement (mean 344.5±12.9 HU) in all patients of this group. At this point attention should be paid to the different contrast medium injection protocols, which offer a higher iodine dose in the dual-energy study group. This was necessary due to the comparatively long acquisition times of the split-filter protocol, to still achieve adequate contrast in the pulmonary arteries as well as in the pulmonary capillary bed, with the latter being particularly important to obtain high iodine map quality. Despite the higher iodine influx rate, HU numbers in the pulmonary trunk were higher in the single-energy group, which was at least partly due to the ATVS (median tube voltage selection of 100 kV) applied in the single-energy group. In contrast, the dual-energy study group showed significantly higher SNR and CNR compared to the single-energy study group, which was mainly due to a comparatively low image noise in the dual-energy study group. However, the dual-energy protocol was associated with a significant increase in SSDE amounting to 26.7%. On the other hand, Euler *et al.* found a 17% decrease in the SSDE (at similar noise levels) within their thoracoabdominal SF-DECT patient cohort. Therefore they postulate that the split-filter technique can be applied without any radiation dose penalty, and might even offer improvements in dose efficiency (22).

Besides providing morphological information about the presence of endoluminal thrombus, the dual-energy technique is capable to provide additional functional information by means of iodine distribution maps (shown in *Figure 4*) and the calculation of lung perfused blood volume (PBV) (28,29). Another possible advantage of dual-energy scanning is the possibility to create virtual monoenergetic images (VMI) as described by others (30-34). Thereby, the dual-energy technique allows for creation of virtual monochromatic images at a low kV energy in CT examinations with suboptimal enhancement of the pulmonary vasculature, thus possibly increasing diagnostic performance for PE detection. In this first investigation

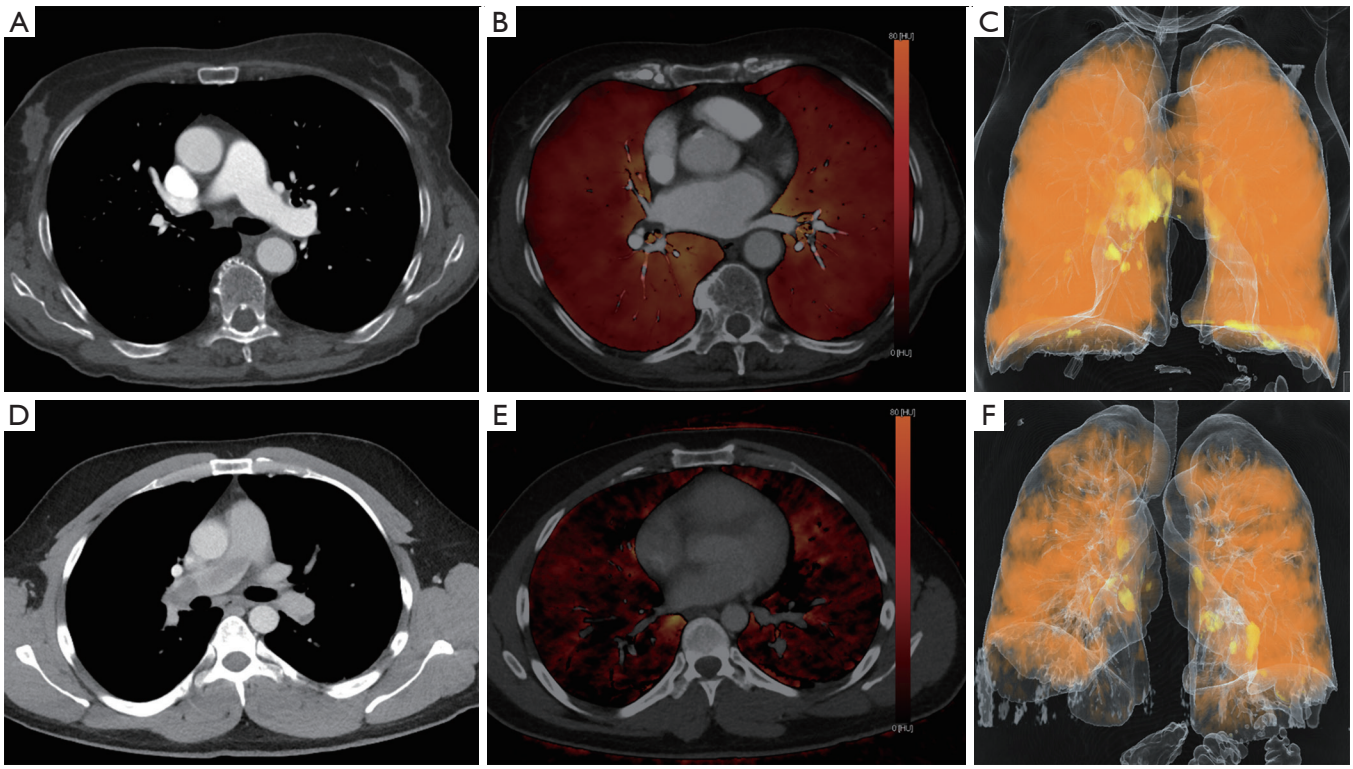

Figure 4 Split-filter dual-energy CTPA of two different patients. A 77-year-old female revealing normal findings in the blended axial (A) standard images, the axial (B) color-coded iodine map, and the coronal (C) VRT. A 39-year-old male demonstrates bilateral central pulmonary embolism in the blended axial (D) standard images, with corresponding diffuse perfusion defects in the axial (E) iodine map and the coronal (F) VRT. CTPA, computed tomography pulmonary angiography; VRT, volume rendering technique.

of SF-DECT for diagnosis of PE, our main focus was based on feasibility of PE image acquisition with the given technical settings. Therefore we choose not to include diagnostic workup of different virtual monoenergetic levels in the present study and instead used the blended 120 kVp equivalents. However, for future investigations, workup of VMI will be of interest. Whether the potential advantage of creating VMI-datasets and iodine distribution maps outweighs a certain dose penalty has to be judged on a case-by-case basis.

The tin component of the new split-filter is responsible for absorption of undesirable low-energy photons which usually do not significantly contribute to the detector signal. The polychromatic X-ray spectrum is thereby shifted towards higher photon energies, which is known as spectral shaping (22,35,36). Moreover, this leads to lower image noise of the split-filter protocol at concurrently preserved image quality when compared to standard single-energy CT (23). Our study results expand the existing body of dual-energy CTPA and thoracic spectral shaping studies, which is so far mainly based on dual-source, dual-layer or rapid kVp switching CT systems (14,36-39).

It seems worth to mention, that technical single-source solutions with the option to offer dual-energy acquisitions are usually available at considerably lower financial expenses compared to the top product spectrum of dual-energy scanners of various vendors. This can be of special interest for primary care hospitals or non-academic facilities aiming at establishing cost-effective dual-energy options.

Discussing the limitations of this work, the effect of SF-DECT on detection of PE was not investigated. However, the promising results from our subjective image quality assessment and observed improvements in SNR/CNR from pulmonary arteries suggest, that this technical approach could also facilitate optimized thrombus detection. Moreover, the dedicated evaluation of split-filter iodine map quality as well as evaluation of virtual monoenergetic reconstructions should be content of

future studies. Although the two study groups show similar clinical characteristics and body habitus, they were not exactly matched. A technical limitation of the SF-DECT technique is the delay between low- and high energy CT data acquisition, which is small but still higher when compared to more established dual-energy techniques such as dual-source, dual-layer detector, or rapid kVp switching CT-systems. Regarding image reconstruction, it has to be mentioned that a model-based iterative reconstruction (IR) algorithm was used (ADMIRE, Siemens). Although IR algorithms nowadays are routinely applied in state-of-the-art cardio-vascular imaging, their exact effect in the environment of dual-energy examinations is still content of ongoing research. However, their potential for further image noise reduction, also in DECT examinations, has been shown before (40). A considerable limitation of the present study is that the scan protocols were applied with the vendor's default settings, which did not offer dose neutrality. On the one hand, the SF-DECT protocol is limited to a fixed tube voltage of 120 kV, while on the other hand, the ATVS applied in the standard single-energy protocol may help facilitate lower dose exposures by applying lower tube voltages. Therefore, a generalizing statement that SF-DECT has a routinely higher dose exposure may be misleading in terms of CTPA. To compensate for different acquisition times, the applied contrast injection protocol was slightly different between study groups, which might have had an impact on pulmonary vessel attenuation and image quality results.

In conclusion, the results of our study suggest that split-filter DECT provides sufficient image quality in the vast majority of patients. However, a value of up to 3.8% non-diagnostic examinations in the current reference standard test for PE is not negligible and raises concerns if this dual-energy protocol in its current form should be recommended for use in clinical routine. The existing opportunity to assess pulmonary "perfusion" based on analysis of iodine distribution maps is associated with higher radiation dose in terms of increased SSDE than conventional single-energy CT with ATVS, with the latter offering the opportunity for potentially dose-saving low kV scanning in appropriate patients.

Acknowledgments

Funding: This publication was supported by the Open Access Publication Fund of the University of Würzburg.

Footnote

Conflicts of Interest: All authors have completed the ICMJE uniform disclosure form (available at http://dx.doi.org/10.21037/qims-20-740). Dr. BP reports personal fees from Siemens Healthcare GmbH and grants from Siemens Healthcare GmbH, outside the submitted work. Dr. AMW reports grants from Siemens Healthcare GmbH, outside the submitted work; Dr. JPG reports personal fees from Siemens Healthcare GmbH, grants from Interdisciplinary Center of Clinical Research Würzburg and grants from Siemens Healthcare GmbH, outside the submitted work; Dr. SV reports grants from Siemens Healthcare GmbH (money payed to the institution), outside the submitted work. Prof. TAB reports grants from Deutsche Forschungsgesellschaft, grants from Siemens Healthcare GmbH, personal fees from Roche/Chugai, personal fees from Novartis, outside the submitted work. The other authors have no conflicts of interest to declare.

Ethical Statement: This Health Insurance Portability and Accountability Act (HIPAA) compliant study was approved by our institutional review board (IRB). Since all CT-scans were clinically indicated the need for individual informed consent was waived by the IRB. The institutional review board approved this study.

References

1. Tapson VF. Acute pulmonary embolism. N Engl J Med 2008;358:1037-52.
2. Ota M, Nakamura M, Yamada N, Yazu T, Ishikura K, Hiraoka N, Tanaka H, Fujioka H, Isaka N, Nakano T. Prognostic significance of early diagnosis in acute pulmonary thromboembolism with circulatory failure. Heart Vessels 2002;17:7-11.
3. Dauphine C, Omari B. Pulmonary embolectomy for acute massive pulmonary embolism. Ann Thorac Surg

2005;79:1240-4.
4. Remy-Jardin M, Pistolesi M, Goodman LR, Gefter WB, Gottschalk A, Mayo JR, Sostman HD. Management of suspected acute pulmonary embolism in the era of CT angiography: a statement from the Fleischner Society. Radiology 2007;245:315-29.
5. Stein PD, Fowler SE, Goodman LR, Gottschalk A, Hales CA, Hull RD, Leeper KV Jr, Popovich J Jr, Quinn DA, Sos TA, Sostman HD, Tapson VF, Wakefield TW, Weg JG, Woodard PK; PIOPED II Investigators. Multidetector Computed Tomography for Acute Pulmonary Embolism. N Engl J Med 2006;354:2317-27.
6. Schaefer-Prokop C, Prokop M. CTPA for the diagnosis of acute pulmonary embolism during pregnancy. Eur Radiol 2008;18:2705-8.
7. Konstantinides SV, Torbicki A, Agnelli G, Danchin N. 2014 ESC guidelines on the diagnosis and management of acute pulmonary embolism. Eur Heart J 2014;35:3033-69,3069a-69k.
8. Johnson TRC. Dual-energy CT: general principles. AJR Am J Roentgenol 2012;199:S3-8.
9. Thieme SF, Graute V, Nikolaou K, Maxien D, Reiser MF, Hacker M, Johnson TR. Dual Energy CT lung perfusion imaging--correlation with SPECT/CT. Eur J Radiol 2012;81:360-5.
10. Thieme SF, Becker CR, Hacker M, Nikolaou K, Reiser MF, Johnson TRC. Dual energy CT for the assessment of lung perfusion--correlation to scintigraphy. Eur J Radiol 2008;68:369-74.
11. Johnson TR, Krauss B, Sedlmair M, Grasruck M, Bruder H, Morhard D, Fink C, Weckbach S, Lenhard M, Schmidt B, Flohr T, Reiser MF, Becker CR. Material differentiation by dual energy CT: initial experience. Eur Radiol 2007;17:1510-7.
12. Siegel MJ, Kaza RK, Bolus DN, Boll DT, Rofsky NM, De Cecco CN, Foley WD, Morgan DE, Schoepf UJ, Sahani DV, Shuman WP, Vrtiska TJ, Yeh BM, Berland LL. White Paper of the Society of Computed Body Tomography and Magnetic Resonance on Dual-Energy CT, Part 1: Technology and Terminology. J Comput Assist Tomogr 2016;40:841-5.
13. Rajiah P, Tanabe Y, Partovi S, Moore A. State of the art: utility of multi-energy CT in the evaluation of pulmonary vasculature. Int J Cardiovasc Imaging 2019;35:1509-24.
14. Weidman EK, Plodkowski AJ, Halpenny DF, Hayes SA, Perez-Johnston R, Zheng J, Moskowitz C, Ginsberg MS. Dual-Energy CT Angiography for Detection of Pulmonary Emboli: Incremental Benefit of Iodine Maps. Radiology 2018;289:546-53.
15. Fink C, Johnson TR, Michaely HJ, Morhard D, Becker C, Reiser M, Nikolaou K. Dual-energy CT angiography of the lung in patients with suspected pulmonary embolism: initial results. Rofo 2008;180:879-83.
16. Bauer RW, Kerl JM, Weber E, Weisser P, Korkusuz H, Lehnert T, Jacobi V, Vogl TJ. Lung perfusion analysis with dual energy CT in patients with suspected pulmonary embolism--influence of window settings on the diagnosis of underlying pathologies of perfusion defects. Eur J Radiol 2011;80:476-82.
17. Pontana F, Faivre JB, Remy-Jardin M, Flohr T, Schmidt B, Tacelli N, Pansini V, Remy J. Lung perfusion with dual-energy multidetector-row CT (MDCT): feasibility for the evaluation of acute pulmonary embolism in 117 consecutive patients. Acad Radiol 2008;15:1494-504.
18. Petritsch B, Kosmala A, Gassenmaier T, Weng AM, Veldhoen S, Kunz AS, Bley TA. Diagnosis of Pulmonary Artery Embolism: Comparison of Single-Source CT and 3rd Generation Dual-Source CT using a Dual-Energy Protocol Regarding Image Quality and Radiation Dose. Rofo 2017;189:527-36.
19. Schenzle JC, Sommer WH, Neumaier K, Michalski G, Lechel U, Nikolaou K, Becker CR, Reiser MF, Johnson TR. Dual energy CT of the chest: how about the dose? Invest Radiol 2010;45:347-53.
20. Hoey ET, Gopalan D, Ganesh V, Agrawal SK, Qureshi N, Tasker AD, Clements L, Screaton NJ. Dual-energy CT pulmonary angiography: a novel technique for assessing acute and chronic pulmonary thromboembolism. Clin Radiol 2009;64:414-9.
21. Rutt B, Fenster A. Split-filter computed tomography: a simple technique for dual energy scanning. J Comput Assist Tomogr 1980;4:501-9.
22. Euler A, Parakh A, Falkowski AL, Manneck S, Dashti D, Krauss B, Szucs-Farkas Z, Schindera ST. Initial Results of a Single-Source Dual-Energy Computed Tomography Technique Using a Split-Filter: Assessment of Image Quality, Radiation Dose, and Accuracy of Dual-Energy Applications in an In Vitro and In Vivo Study. Invest Radiol 2016;51:491-8.
23. Euler A, Obmann MM, Szucs-Farkas Z, Mileto A, Zaehringer C, Falkowski AL, Winkel DJ, Marin D, Stieltjes B, Krauss B, Schindera ST. Comparison of image quality and radiation dose between split-filter dual-energy images and single-energy images in single-source abdominal CT. Eur Radiol 2018;28:3405-12.
24. May MS, Wiesmueller M, Heiss R, Brand M, Bruegel J,

Uder M, Wuest W. Comparison of dual- and single-source dual-energy CT in head and neck imaging. Eur Radiol 2019;29:4207-14.
25. Boone JM, Strauss KJ, Cody DD, McCollough CH, McNitt-Gray MF, Toth TL. Size-Specific Dose Estimates In Pediatric and Adult Body CT Examinations: Report No. 204. American Association of Physicists in Medicine, Coll Park; 2011.
26. Sullivan GM, Artino AR. Analyzing and Interpreting Data From Likert-Type Scales. J Grad Med Educ 2013;5:541-42.
27. Koo TK, Li MY. A Guideline of Selecting and Reporting Intraclass Correlation Coefficients for Reliability Research. J Chiropr Med 2016;15:155-63.
28. Okada M, Kunihiro Y, Nakashima Y, Nomura T, Kudomi S, Yonezawa T, Suga K, Matsunaga N. Added value of lung perfused blood volume images using dual-energy CT for assessment of acute pulmonary embolism. Eur J Radiol 2015;84:172-7.
29. Sueyoshi E, Tsutsui S, Hayashida T, Ashizawa K, Sakamoto I, Uetani M. Quantification of lung perfusion blood volume (lung PBV) by dual-energy CT in patients with and without pulmonary embolism: preliminary results. Eur J Radiol 2011;80:e505-9.
30. Delesalle MA, Pontana F, Duhamel A, Faivre JB, Flohr T, Tacelli N, Remy J, Remy-Jardin M. Spectral optimization of chest CT angiography with reduced iodine load: experience in 80 patients evaluated with dual-source, dual-energy CT. Radiology 2013;267:256-66.
31. Apfaltrer P, Sudarski S, Schneider D, Nance JW Jr, Haubenreisser H, Fink C, Schoenberg SO, Henzler T. Value of monoenergetic low-kV dual energy CT datasets for improved image quality of CT pulmonary angiography. Eur J Radiol 2014;83:322-8.
32. Almutairi A, Al Safran Z, AlZaabi SA, Sun Z. Dual energy CT angiography in peripheral arterial stents: optimal scanning protocols with regard to image quality and radiation dose. Quant Imaging Med Surg 2017;7:520-31.
33. Hickethier T, Baeßler B, Kroeger JR, Doerner J, Pahn G, Maintz D, Michels G, Bunck AC. Monoenergetic reconstructions for imaging of coronary artery stents using spectral detector CT: In-vitro experience and comparison to conventional images. J Cardiovasc Comput Tomogr 2017;11:33-9.
34. Di Maso LD, Huang J, Bassetti MF, DeWerd LA, Miller JR. Investigating a novel split-filter dual-energy CT technique for improving pancreas tumor visibility for radiation therapy. J Appl Clin Med Phys 2018;19:676-83.
35. Haubenreisser H, Meyer M, Sudarski S, Allmendinger T, Schoenberg SO, Henzler T. Unenhanced third-generation dual-source chest CT using a tin filter for spectral shaping at 100kVp. Eur J Radiol 2015;84:1608-13.
36. Gordic S, Morsbach F, Schmidt B, Allmendinger T, Flohr T, Husarik D, Baumueller S, Raupach R, Stolzmann P, Leschka S, Frauenfelder T, Alkadhi H. Ultralow-dose chest computed tomography for pulmonary nodule detection: first performance evaluation of single energy scanning with spectral shaping. Invest Radiol 2014;49:465-73.
37. Braun FM, Johnson TRC, Sommer WH, Thierfelder KM, Meinel FG. Chest CT using spectral filtration: radiation dose, image quality, and spectrum of clinical utility. Eur Radiol 2015;25:1598-606.
38. Petritsch B, Kosmala A, Weng AM, Bley TA. Tin-filtered 100 kV ultra-low-dose CT of the paranasal sinus: Initial clinical results. PLoS One 2019;14:e0216295.
39. Ghandour A, Sher A, Rassouli N, Dhanantwari A, Rajiah P. Evaluation of Virtual Monoenergetic Images on Pulmonary Vasculature Using the Dual-Layer Detector-Based Spectral Computed Tomography. J Comput Assist Tomogr 2018;42:858-65.
40. Landry G, Gaudreault M, van Elmpt W, Wildberger JE, Verhaegen F. Improved dose calculation accuracy for low energy brachytherapy by optimizing dual energy CT imaging protocols for noise reduction using sinogram affirmed iterative reconstruction. Z Med Phys 2016;26:75-87.

Cite this article as: Petritsch B, Pannenbecker P, Weng AM, Grunz JP, Veldhoen S, Bley TA, Kosmala A. Split-filter dual-energy CT pulmonary angiography for the diagnosis of acute pulmonary embolism: a study on image quality and radiation dose. Quant Imaging Med Surg 2021;11(5):1817-1827. doi: 10.21037/qims-20-740

